# Domino-Redox Reaction Induced by An Electrochemically Triggered Conformational Change

Takashi Harimoto,[a] Tomoki Tadokoro,[a] Soichiro Sugiyama,[a] Takanori Suzuki[a] and Yusuke Ishigaki*[a]

[a] Mr. T. Harimoto, Mr. T. Tadokoro, Mr. S. Sugiyama, Prof. Dr. T. Suzuki, Prof. Dr. Y, Ishigaki
Department of Chemistry, Faculty of Science
Hokkaido University
N10 W8, North-ward, Sapporo 060-0810, Japan
E-mail: yishigaki@sci.hokudai.ac.jp

**Abstract:** The concept of a domino-type reaction has been applied in a wide range of fields such as synthetic organic chemistry, material engineering, and life science. To extend the domino concept to redox chemistry, we designed and synthesized a dimeric quinodimethane (QD) with a nonplanar dithiin spacer. The domino-redox properties can be activated by raising the temperature, based on a thermally equilibrated twisted conformation of QD, which has a higher highest occupied molecular orbital (HOMO) level that is more readily oxidized. After one QD unit is oxidized (trigger), steric repulsion and electronic interaction between electrophores make the neighboring QD unit adopt a twisted conformation (domino process), which facilitates the following oxidation. Thus, a domino-redox reaction was achieved for the first time by a change in the HOMO level due to a drastic change in the molecular conformation.

## Introduction

Domino reactions are intramolecular reactions in which a single event triggers the conversion of a starting material to a product, which then provides a substrate for the next reaction until a stable final product is obtained (Figure 1a).[1–8] They have contributed greatly to green chemistry such as by improving the reaction efficiency (atom economy) and simplifying the workup process, thanks to the generation of multiple bonds in a single step. However, it can be difficult to apply the concept of domino reactions to redox reactions due to electrostatic reasons (Figure 1b),[9–13] since in general, an electron transfer (ET) reaction produces a positively or negatively charged species. As a result, the oxidation/reduction reaction proceeds in a stepwise manner with an anodic/cathodic shift of the electric potential for the subsequent process.[14]

One of the exceptions is the “dyrex (dynamic redox)” system,[15] such as tetraarylanthraquinodimethane (AQD, **A**), in which the first oxidation of **A** with a folded geometry generates $\mathbf{A}^{+\bullet}$ that undergoes a rapid structural change into $(\mathbf{A'})^{+\bullet}$ with a twisted geometry (Figure 2 and Scheme S1). Since $(\mathbf{A'})^{+\bullet}$ (twisted) is more easily oxidized than $\mathbf{A}^{+\bullet}$ (folded) or even than **A** (folded), the second oxidation occurs nearly at the same potential to generate $(\mathbf{A'})^{2+}$ (twisted). This process is akin to the domino process, however, **A** could undergo only two-electron (2e) oxidation, and thus the first ET only facilitates the second ET but could not continue the process, so that it is not a domino process. In addition, organic systems constructed by the assembly of multiple redox-active units (electrophores) are attracting much attention since it could exhibit superior charge transport properties based on their potential to interconvert with multivalent ionic species.[16–28]

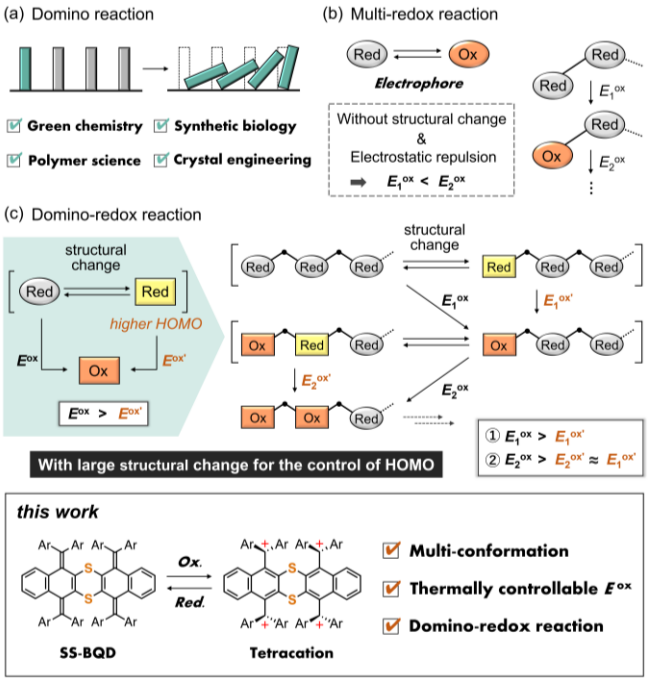


**Figure 1.** (a) The concept of domino reactions. (b) General scheme for multi-redox reaction without a change in structure of electrophore. (c) This work for realizing domino-redox reaction by a large change in structure of electrophore after oxidation of the neighboring unit.

To realize domino-redox reactions in multi-redox systems consisting of the same kinds of electrophores, some novel mechanism is necessary, so that the initial redox reaction in one electrophore facilitates the subsequent redox reaction of the neighboring unit (Figure 1c and Schemes S3 and S4). As the simplest model of the multi-chromophoric systems, we recently studied octaarylbisquinodimethane (BQD) derivatives **B**, which have two units of the folded-shaped AQD connected by a rigid π-linker (Figure 2 and Scheme S2).[29] If they exhibit the domino process, the same idea could be applied for the much larger multi-redox systems to facilely generate oligo/poly-cations. In fact, **B** underwent one-wave four-electron (4e) oxidation to give tetracation $\mathbf{B}^{4+}$, however, this did not lead to the domino-redox reaction, because the oxidation potential of **B** is similar to that of monomeric AQD **A** with the same aryl groups,[15,30–32] which

undergoes one-wave 2e-oxidation. Thus, the oxidation behavior of multi-redox system **B** could instead be explained by the independent ET process of two quinodimethane (QD) units. To achieve a domino-type redox reaction, mutual steric repulsion and/or electronic interaction between the electrophores is important, while it is prevented due to rigidity of the spacer in **B**.

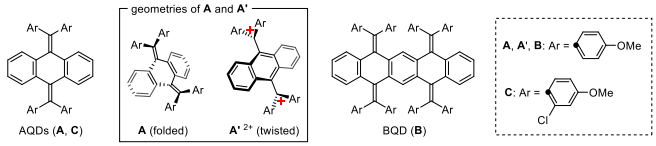


**Figure 2.** Related compounds **A**/**A**', **B**, and **C**.

Thus, we anticipated that, instead of fusing the QD units with a rigid π-skeleton, bridging two electrophores with a more flexible nonplanar linker would be promising. We chose the dithiin skeleton, which was used to construct several nanohoops and nanobelts.[33–35] Herein, we newly designed SS-BQD **1**, which consists of two QD units fused with a dithiin skeleton. The backbone of SS-BQD **1** is expected to exhibit higher flexibility, allowing close proximity of two QD units for mutual communication, thus affecting the structural preference of a QD unit while adopting one of multiple conformations, such as folded (**F**) and twisted (**T**) forms, with different electronic structures. In many cases, the AQD electrophore prefers the folded form with a low highest occupied molecular orbital (HOMO) level whereas the high-energy twisted form has a much higher HOMO.[15]

A detailed investigation of the effects of changes in the conformation of QD units on the redox behavior indicated that, after the initial oxidation of SS-BQD, subsequent oxidation of the second unit is facilitated by raising the HOMO level, which is caused by a dynamic change in conformation of the intermediary dicationic state. In addition, this domino process could be clearly demonstrated since the initial oxidation process of the neutral species is activated by raising the temperature through the thermal equilibrium among the conformers in SS-BQD, thanks to the redox properties of a QD unit being drastically modified by adopting the less stable twisted form. In this paper, we report the first example of a domino-redox reaction induced by a drastic change in conformation that is accompanied by a domino-type change in the HOMO level.

## Results and Discussion

To construct SS-BQD-based redox systems, we selected a 4-methoxyphenyl group as the aryl group, since it has enough electron-donating ability to stabilize the cationic states. By an eight-fold Suzuki-Miyaura cross-coupling reaction, SS-BQD **1a** with 4-methoxyphenyl groups was prepared in 92% yield in a one-step manner from tetrakis(dibromomethylene) precursor **3**, which was prepared from tetraone **2**[36] (Figure 3a). In addition, to investigate the effect of a restricted change in the structure of the QD unit,[32] we prepared the reference compound **1b** with a chlorine atom at the 2-position of the 4-methoxyphenyl group in a similar manner (56%).

X-ray analysis of SS-BQD **1a** using a benzene-solvated single crystal obtained by recrystallization from benzene/hexane showed that SS-BQD **1a** contains two units of folded QD, which are connected by a boat-shaped dithiin spacer (Figure 3b). Thus, **1a** adopts a U-shaped conformation (**F-F**$_{syn}$) in which the concave faces of the QD units are directed to the same sides. On the other hand, X-ray analysis of a $CHCl_3$-solvated single crystal obtained from $CHCl_3$/hexane revealed that SS-BQD **1a** adopts a Z-shaped conformation (**F-F**$_{anti}$) with the two folded QD units (Figure 3c), while their concave faces are directed to the opposite side. These results clearly show that two conformers with QD units in different orientations can exist as stable species in the crystals. The observation of both conformers by X-ray analysis indicated that **1a** exists in a state of rapid equilibrium of the **F-F**$_{syn}$ and **F-F**$_{anti}$ conformations in solution.

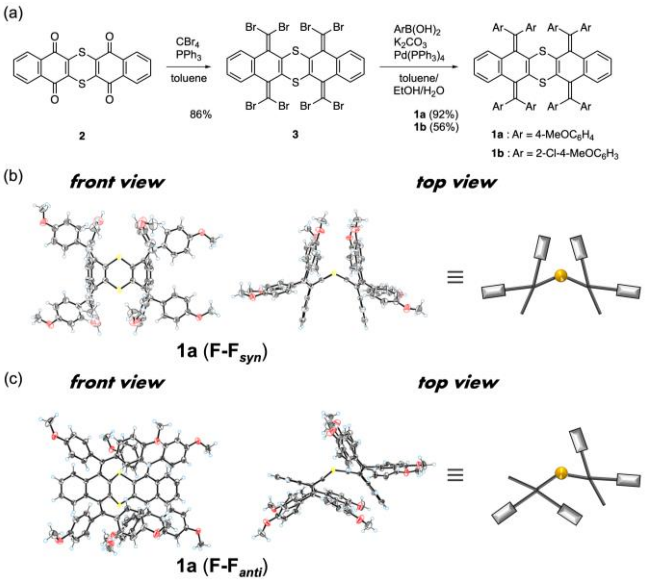


**Figure 3.** (a) Preparation of newly designed SS-BQDs **1**. X-ray crystal structures (ORTEP drawings) of (b) **1a** (**F-F**$_{syn}$)[#] and (c) **1a** (**F-F**$_{anti}$) determined at 150 K. The solvent molecules and disordered atoms are omitted for clarity. Thermal ellipsoids are shown at the 50% probability level. [#]One of the two crystallographically independent molecules.

Thanks to the electron-donating nature of the 4-methoxyphenyl and 2-chloro-4-methoxyphenyl groups, upon treatment of **1a** and **1b** with four equivalents of $(4\text{-}BrC_6H_4)_3N^{+\bullet}SbCl_6^-$, the tetracation salts **1a**$^{4+}$$(SbCl_6^-)_4$ and **1b**$^{4+}$$(SbCl_6^-)_4$ were obtained quantitatively (Figure 4). When the tetracations **1a**$^{4+}$ and **1b**$^{4+}$ were reduced with Zn powder, the neutral species **1a** and **1b** were recovered quantitatively. X-ray analysis of tetracation salt **1a**$^{4+}$$(SbCl_6^-)_4$ showed that tetracation adopts almost orthogonally twisted structures, with large dihedral angles between the central pentacyclic skeleton and each diarylmethylium unit [64.7(8)° - 82.3(8)°] (Table S4). These results indicate that the tetracation adopts a perpendicular geometry, whereas the QD units in the neutral state prefer a folded geometry.

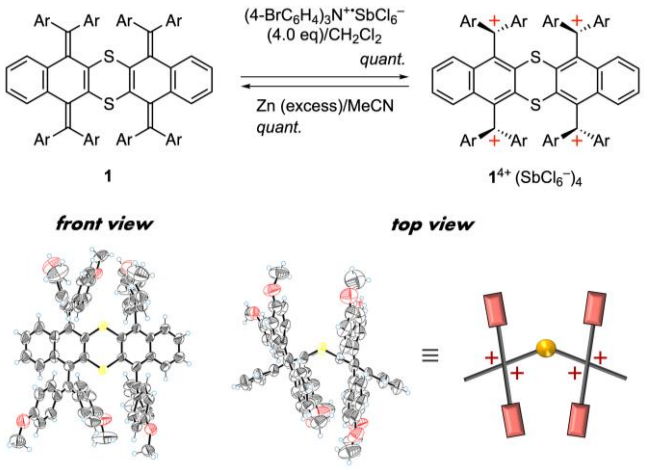


**Figure 4.** Redox interconversion between neutral donors and tetracations. Four equivalents of $(4\text{-}BrC_6H_4)_3N^{+\bullet}SbCl_6^-$ were used for the oxidation of **1a** and **1b**, respectively. X-ray crystal structures (ORTEP drawings) of $\mathbf{1a}^{4+}(SbCl_6^-)_4$ determined at 100 K. The counterions, solvent molecules, and disordered atoms are omitted for clarity. Thermal ellipsoids are shown at the 50% probability level.

Such a change in structures between the neutral and cationic states are common with AQD derivatives **A** and **C**,[15,32] which is reflected in the redox behavior with large separation of the oxidation and reduction peaks (Figure S36). This would also be the case for SS-BQD. Indeed, a cyclic voltammogram of **1b** in $CH_2Cl_2$ exhibited one-wave 4e-redox peaks at quite different potentials, each of which corresponds to the oxidation of **1b** and the reduction of $\mathbf{1b}^{4+}$, respectively (Figure 5). The redox behaviors of **A** and **1b** do not change when measured at other scan rates or at other temperatures (Figures S37-S40). However, quite different and rather reversible redox waves were observed for **1a** at 298 K. A cathodic shift of the oxidation wave compared to that of AQD **A** with 4-methoxyphenyl groups suggests that **1a** has a much higher HOMO than AQD **A** (Figure S36).

The nearly reversible redox waves imply that there is almost no change in structure between before and after the oxidation of neutral species **1a** in solution. Considering that tetracation $\mathbf{1a}^{4+}$ only adopts a perpendicularly twisted structure as suggested by an X-ray analysis, NMR (Figure S4) and UV-Vis spectra (Figure S29b), and theoretical calculations (*vide infra*), the oxidation of neutral species **1a** should occur from the conformations other than those observed in crystal by X-ray, so that one or both of the two QD units adopt a twisted-form.

We considered that a more stable folded form and a metastable twisted form in the QD units of **1a** would be in thermal equilibrium at 298 K. To validate this hypothesis, the cyclic voltammogram was measured at 195 K in $CH_2Cl_2$. As expected from the general view that the metastable form makes less of a contribution at a lower temperature, the voltammogram showed a large separation of redox peaks, indicating that the QD units with a folded form are dominant in solution at 195 K, and thus a large change in structure between the neutral donor and the tetracation was indicated (Figure 5). A continuous change was observed by measuring the voltammogram of **1a** at different temperatures between 195 K and 298 K (Figures 6a and S41). Similarly, when the scan rate was increased during the measurements at 298 K, the similar continuous change was observed showing large separation of redox peaks at higher scan speeds (Figures 6b and S42). The above results show that the less populated but easily-oxidized form is supplied from the most stable forms at higher temperature and/or at slower scan rate.

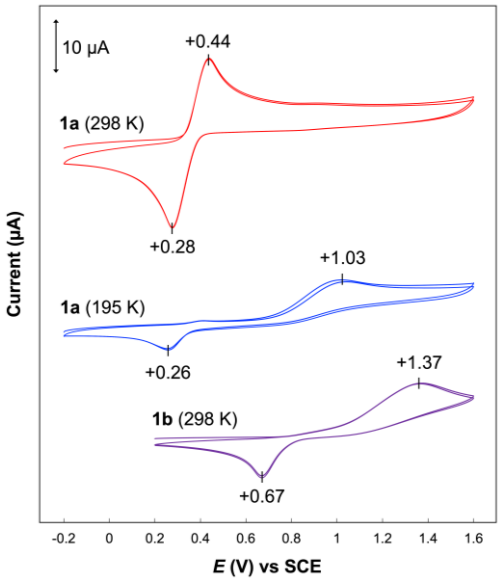


**Figure 5.** Cyclic voltammograms of SS-BQDs **1a** and **1b** in $CH_2Cl_2$ containing 0.1 M $Bu_4NBF_4$ as a supporting electrolyte (scan rate 100 mV $s^{-1}$, Pt electrodes). [**1a**: Ar = 4-$MeOC_6H_4$; **1b**: Ar = 2-Cl-4-$MeOC_6H_3$]

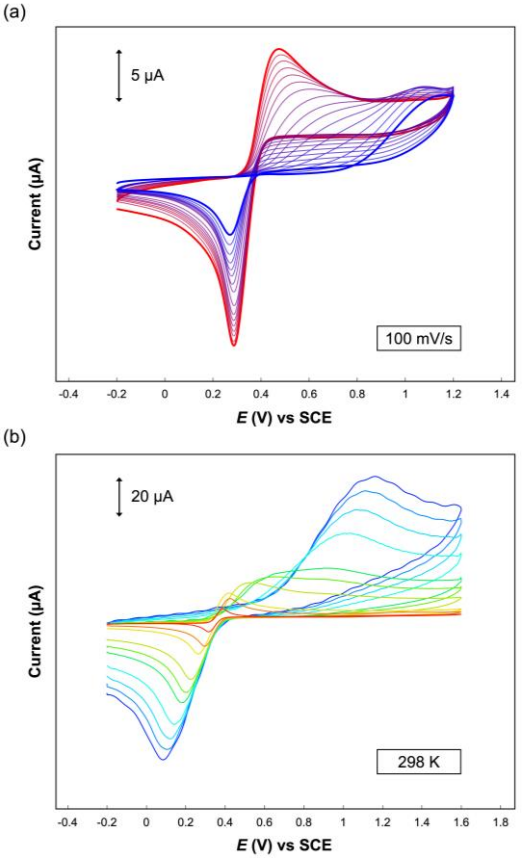


**Figure 6.** Cyclic voltammograms of SS-BQD **1a** in $CH_2Cl_2$ containing 0.1 M $Bu_4NBF_4$ as a supporting electrolyte (Pt electrodes). (a) Measured at various temperatures varied continuously from 195 K (blue) to 298 K (red). (b) Measured at various scan rates varied from 10 mV $s^{-1}$ (red) to 5 V $s^{-1}$ (blue).

Based on the thermally activatable redox behavior observed in SS-BQD **1a**, we can propose a mechanism for the redox process shown in Scheme 1. The two conformers **F-F**$_{syn}$ and **F-F**$_{anti}$, in

which both QD units adopt the folded form, are in equilibrium in solution via the rapid flipping motion of QD units. At 195K, the voltammogram of **1a** is similar to that of **1b**, in the latter of which the twisted QD unit does not need to be considered due to the substituents at the 2-position of aryl groups even at 298 K. These results indicate that the contribution of the metastable conformation with a twisted QD unit of **1a** is negligibly small at lower temperatures.

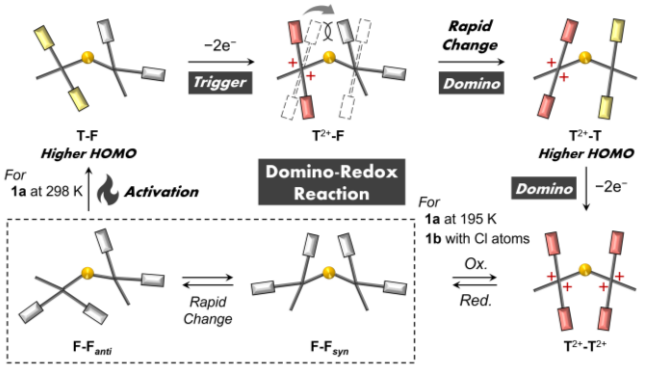


**Scheme 1.** A plausible mechanism for domino-redox reaction induced by an electrochemically triggered conformational change.

When the temperature was raised to 298 K, some contribution from the conformer containing a twisted QD unit (e.g., **T-F**) is expected with a change in redox behavior. While its proportion should be small, the high HOMO of the **T-F** conformer allows facile oxidation of **1a** since **F-F*syn*** and **F-F*anti*** are in rapid equilibrium with **T-F**. After the **T-F** conformer undergoes an apparent 2e-oxidation, the as-generated dication **1a**$^{2+}$ adopts the **T**$^{2+}$**-F** conformation, which has a twisted bis(diarylmethylium) moiety and the neutral QD unit of the folded form. Importantly, due to the steric repulsion between electrophores, the folded QD unit in the dication **1a**$^{2+}$ could further undergo a rapid change in conformation into the twisted QD, with the formation of a doubly twisted conformer **T**$^{2+}$**-T** with a higher HOMO level than **T**$^{2+}$**-F** (Figures 7b, S13, and S24). Moreover, in the **T**$^{2+}$**-T** conformers, the HOMO and lowest unoccupied molecular orbital (LUMO) are delocalized in the orthogonally attached diarylmethylene/methylium units, suggesting the presence of interelectrophore interactions. In this way, the change in conformation can facilitate subsequent 2e-oxidation so that it happens at nearly the same potential as for **T-F**, resulting in the formation of tetracation **1a**$^{4+}$ with the **T**$^{2+}$**-T**$^{2+}$ conformation.

This scenario for the domino-redox reaction is most likely to account for the one-wave 4e-oxidation process of **1a** at the cathodically shifted potential compared to AQD **A**. The change in conformation of the as-generated **1a**$^{2+}$ is the key for the success of the domino process. The **T**$^{2+}$**-F** conformer of **1a**$^{2+}$ generated by the initial oxidation exhibits steric repulsion between two electrophores as in the case of neutral **T-F**. However, the repulsion in the dicationic state cannot be released as in the neutral state, since the **T**$^{2+}$ part cannot convert to the folded form. The only way to relieve the repulsion in **T**$^{2+}$**-F** is by a change in the conformation of the QD unit to the twisted form, which warrants the downstream change in conformation from **T**$^{2+}$**-F** to **T**$^{2+}$**-T**. When a spectral change was followed by UV-Vis spectroscopy upon electrochemical oxidation in $CH_2Cl_2$, a clean conversion of **1a** to tetracation **1a**$^{4+}$ (Figure S31) were observed with isosbestic points at 314 and 347 nm. At the early-stage of oxidation, a slightly red-shifted absorption maximum (529 nm) was observed, which merged into the absorption of **1a**$^{4+}$ at 507 nm, suggesting that the dicationic intermediate could be transiently detected under the constant-current electrolytic condition. Then, to observe transient dication **1a**$^{2+}$ more clearly, we conducted electrochemical oxidation of **1a** in MeCN, which can stabilize the intermediary cationic species by an effective solvation. Indeed, stepwise oxidation processes were observed via the intermediary dication (Figure S32) with several isosbestic points in each oxidation process, indicating that the transient **T**$^{2+}$**-F** form can be long-lived in MeCN, which was supported by DFT calculations (Table S1).

To validate the domino-redox scenario by evaluating the relative energies ($E_{rel}$) of the conformers, DFT calculations were performed at the B3LYP-D3/6-31G* level. Since the VT-NMR measurements (*vide infra*) did not show any biradical character, open-shell species would be energetically overestimated and can be excluded. The results showed that not only the **F-F*syn*** and **F-F*anti*** conformations with folded QD units but also the **T-F** conformation with a twisted QD unit were obtained as energy-minimized structures for **1a** (Figures 7a and S12). The energy difference between **F-F*syn*** and **F-F*anti*** (3.19 kcal/mol) suggests that there is some steric repulsion/dispersion attraction between electrophores over the dithiin skeleton. The **T-F** conformer with a higher HOMO level has an $E_{rel}$ value of 5.90 kcal/mol, which is small enough to consider the contribution from this conformer with an increase in temperature. On the other hand, the **T-T** conformer is much less stable ($E_{rel}$: 20.2 kcal/mol), so the contribution of the **T-T** conformer is negligible (Figure S12 and Table S1). In the case of dication **1a**$^{2+}$, the **T**$^{2+}$**-T** form is more stable than **T**$^{2+}$**-F** ($E_{rel}$: 6.76 kcal/mol), as discussed above based on the interelectrophore interaction (Figures 7b and S13). Again, the **T**$^{2+}$**-T** form has a higher HOMO than **T**$^{2+}$**-F** (Figure S24), indicating that subsequent oxidation of **1a**$^{2+}$ to **1a**$^{4+}$ would readily occur to accomplish the domino-redox reaction.

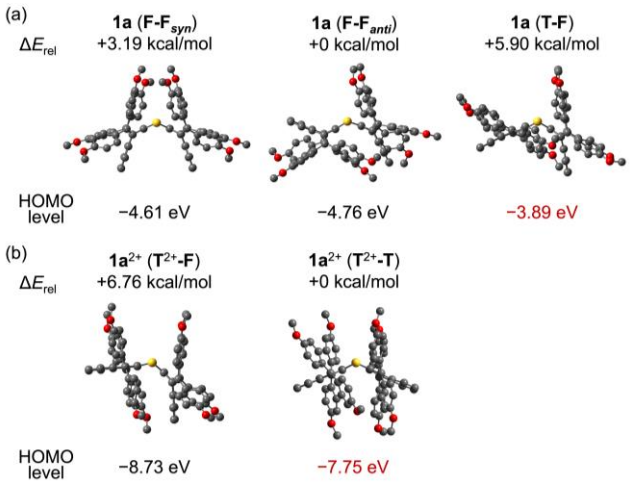


**Figure 7.** Optimized structures of possible isomers of (a) **1a** and (b) **1a**$^{2+}$ obtained by DFT calculations at the B3LYP-D3/6-31G* level. Hydrogen atoms are omitted for clarity.

On the other hand, the calculation for **1b** with a 2-chloro substituent on the aryl group showed a considerable change in the relative stability of conformers. In the neutral state, we tried to find other conformations with a twisted QD unit, but both the **T-T** and **T-F** conformations were not obtained as energy-minimized structures (Figure S15). Furthermore, in the dicationic state, $\mathbf{T}^{2+}$**-F** conformer should be dominant because of the very large $E_{rel}$ value (17.5 kcal/mol) for the $\mathbf{T}^{2+}$**-T** conformer of $\mathbf{1b}^{2+}$ (Figure S16). These theoretical results can account for the absence of a domino-redox reaction in the reference compound **1b**.

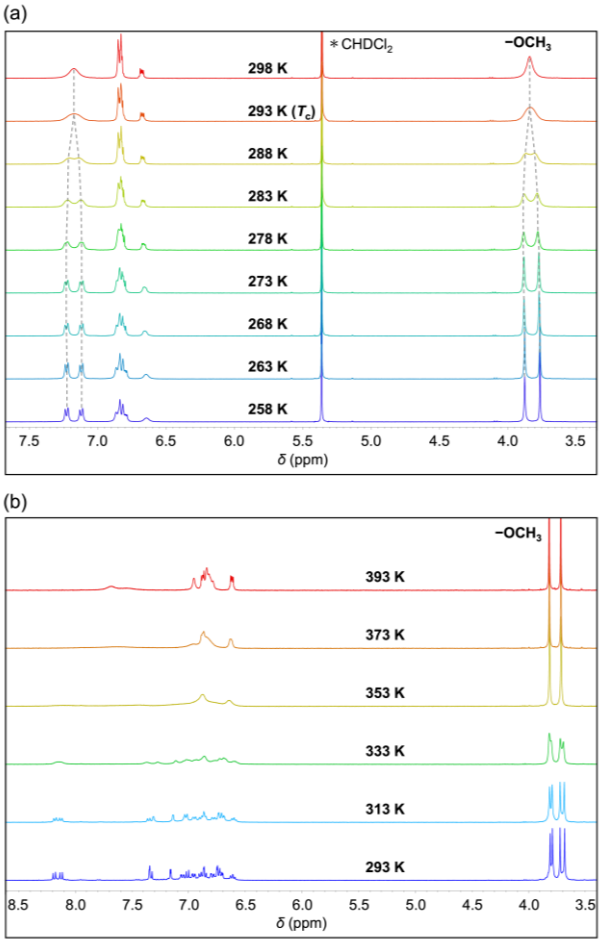


**Figure 8.** VT-$^1$H NMR spectra of (a) **1a** in $CD_2Cl_2$ (193–258 K) and (b) **1b** in DMSO-$d_6$ (293–393 K).

Finally, VT-$^1$H NMR analyses were conducted to evaluate the energy barrier for the interconversion among the conformers in **1a** and **1b**. Although the less-populated conformer (**T-F**) with a twisted QD unit was not detected in the spectrum, the energy barrier for the conversion of **F-F** and **T-F** should be smaller than that for exomethylene rotation. Indeed, the $^1$H NMR spectrum of **1a** at 298 K in $CD_2Cl_2$ showed a single broad signal of the methoxy protons (δ=3.8 ppm) (Figure 8a). Upon cooling to 258 K, the corresponding methoxy signal splits into two sharp signals and their resonances are assigned to a closed-shell species with $C_{2v}$-symmetry; this observation indicates that rotation of the exomethylene bond of SS-BQD **1a** can be suppressed at lower temperatures. Based on the coalescence temperature $T_c$ (293 K) for the methoxy protons on the aryl groups, the $\Delta G^{\neq}$ value was estimated to be 14.6 kcal mol$^{-1}$, which is sufficiently small for free rotation of the exomethylene bond under ambient conditions. At even lower temperatures, the dynamic motion of major **F-F**$_{anti}$ conformer can be suppressed in solution at 193 K due to the slow ring-flip of the dithiin unit for SS-BQD **1a** (Figure S33). Based on the coalescence of aromatic proton signals, the energy barrier $\Delta G^{\neq}$ of the ring-flip was estimated to be 10.1 kcal/mol, suggesting that the ring-flip motion proceeds more easily than rotation of the exomethylene bond for SS-BQD **1a**. In addition, even at higher temperatures in DMSO-$d_6$ (Figure S34), very sharp signals were observed, which suggests that the open-shell character is negligible in SS-BQD **1a**.

In contrast to **1a**, no coalescence of the methoxy proton signals was observed even at 393 K in DMSO-$d_6$ for reference compound **1b** (Figures 8b and S35), suggesting that the introduction of a sterically hindered chlorine atom at the 2-position increases the energy barrier, which prevents free rotation of the exomethylene bond. The difference in the rotational dynamics of the exomethylene bonds between **1a** and **1b** revealed by the above VT-$^1$H NMR analyses should be closely related to the results of electrochemical measurements, in which **1a** exhibited a dynamic change in redox properties, unlike **1b**. Thus, based on the easy rotation of the exomethylene bond of **1a**, the interconversion from **F-F**$_{syn}$ and/or **F-F**$_{anti}$ to the **F-T** conformation would be fully feasible in solution, resulting in the first observation of a domino-redox reaction.

## Conclusion

In conclusion, we designed and synthesized a SS-BQD derivative, in which the redox-active QD units are connected by a nonplanar dithiin skeleton, which allows steric repulsion and/or electronic interaction between electrophores for specific conformers. VT-electrochemical measurements showed that **1a** with a flexible structure exhibits temperature-dependent redox properties, unlike *ortho*-substituted **1b**, which is less flexible. VT-$^1$H NMR measurements revealed that **1a** undergoes a smooth change in conformation, and thus the metastable **T-F** conformer can be partially generated with an increase in temperature (activation), and undergoes facile apparent 2e-transfer (trigger). In the resulting dication $\mathbf{1a}^{2+}$, the steric repulsion and interelectrophore interaction cause a facile change in structure from the as-generated $\mathbf{T}^{2+}$**-F** conformer to the $\mathbf{T}^{2+}$**-T** conformer (domino), which facilitates the subsequent oxidation (domino) to $\mathbf{1a}^{4+}$ of the $\mathbf{T}^{2+}$-$\mathbf{T}^{2+}$ conformer. This is the first successful demonstration of the domino-redox reaction of multi-redox systems consisting of the same kind of electrophores (Schemes 1 and S3). This work presents a new molecular design concept for organic systems containing multiple redox-active units (Scheme S4), so that they can exhibit superior charge transport properties based on facile and nearly simultaneous multiple electron transfer to generate multivalent ionic species.

## Supporting Information

The authors have cited additional references within the Supporting Information.[37–40]

## Acknowledgements

This work was supported by Grant-in-Aid from MEXT and JSPS (Nos. JP20H02719 to T.S. and JP21H01912 and JP23H04011 to Y.I.) and JST PRESTO (JPMJPR23Q1 to Y.I). T.H. and T.T. are grateful for JSPS Grant-in-Aid for Research Fellow JP22KJ0115 and JP23KJ0065, respectively. Y.I. acknowledges the Foundation of the Promotion of Ion Engineering. This work was also supported by the Research Program of “Five-star Alliance” in “NJRC Mater. & Dev.” MEXT.

**Keywords:** Domino reactions • Multi-conformation • Redox systems • Quinodimethanes • X-ray diffraction

[1] L. F. Tietze, *Chem. Rev.* **1996**, *96*, 115–136.

[2] L. F. Tietze (Ed.), *Domino Reactions : Concepts for Efficient Organic Synthesis*, Wiley-VCH, Weinheim, **2014**.

[3] K. C. Nicolaou, T. Montagnon, S. A. Snyder, *Chem. Commun.* **2003**, *3*, 551–564.

[4] K. C. Nicolaou, D. J. Edmonds, P. G. Bulger, *Angew. Chem. Int. Ed.* **2006**, *45*, 7134–7186.

[5] D. Enders, C. Grondal, M. R. M. Hüttl, *Angew. Chem. Int. Ed.* **2007**, *46*, 1570–1581.

[6] A. Grossmann, D. Enders, *Angew. Chem. Int. Ed.* **2012**, *51*, 314–325.

[7] H. Pellissier, *Adv. Synth. Catal.* **2012**, *354*, 237–294.

[8] R. Westphal, E. Venturini Filho, F. Medici, M. Benaglia, S. J. Greco, *Synthesis (Stuttg).* **2022**, *54*, 2927–2975.

[9] K. Deuchert, S. Hünig, *Angew. Chem. Int. Ed. Engl.* **1978**, *17*, 875–886.

[10] T. Nishinaga, *Organic Redox Systems*, John Wiley & Sons, Inc, Hoboken, NJ, **2015**.

[11] G. Kwon, S. Lee, J. Hwang, H.-S. Shim, B. Lee, M. H. Lee, Y. Ko, S.-K. Jung, K. Ku, J. Hong, K. Kang, *Joule* **2018**, *2*, 1771–1782.

[12] J. Shukla, V. P. Singh, P. Mukhopadhyay, *ChemistryOpen* **2020**, *9*, 304–324.

[13] H. Ueda, S. Yoshimoto, *Chem. Rec.* **2021**, *21*, 2411–2429.

[14] D. H. Evans, *Chem. Rev.* **2008**, *108*, 2113–2144.

[15] Y. Ishigaki, K. Sugawara, T. Tadokoro, Y. Hayashi, T. Harimoto, T. Suzuki, *Chem. Commun.* **2021**, *57*, 7201–7214.

[16] K. Katsuma, Y. Shirota, *Adv. Mater.* **1998**, *10*, 223–226.

[17] M. Kivala, C. Boudon, J.-P. Gisselbrecht, P. Seiler, M. Gross, F. Diederich, *Angew. Chem. Int. Ed.* **2007**, *46*, 6357–6360.

[18] J. C. Barnes, A. C. Fahrenbach, D. Cao, S. M. Dyar, M. Frasconi, M. A. Giesener, D. Benítez, E. Tkatchouk, O. Chernyashevskyy, W. H. Shin, H. Li, S. Sampath, C. L. Stern, A. A. Sarjeant, K. J. Hartlieb, Z. Liu, R. Carmieli, Y. Y. Botros, J. W. Choi, A. M. Z. Slawin, J. B. Ketterson, M. R. Wasielewski, W. A. Goddard, J. F. Stoddart, *Science* **2013**, *339*, 429–433.

[19] G. Zhang, V. Lami, F. Rominger, Y. Vaynzof, M. Mastalerz, *Angew. Chem. Int. Ed.* **2016**, *55*, 3977–3981.

[20] S. Dong, T. Y. Gopalakrishna, Y. Han, H. Phan, T. Tao, Y. Ni, G. Liu, C. Chi, *J. Am. Chem. Soc.* **2019**, *141*, 62–66.

[21] W. Nojo, Y. Ishigaki, T. Takeda, T. Akutagawa, T. Suzuki, *Chem. – A Eur. J.* **2019**, *25*, 7759–7765.

[22] C. R. Bridges, A. M. Borys, V. A. Béland, J. R. Gaffen, T. Baumgartner, *Chem. Sci.* **2020**, *11*, 10483–10487.

[23] L. Ueberricke, B. Punja Benke, T. Kirschbaum, S. Hahn, F. Rominger, U. H. F. Bunz, M. Mastalerz, *Chem. – A Eur. J.* **2021**, *27*, 2043–2049.

[24] V. Bliksted Roug Pedersen, J. Granhøj, A. Erbs Hillers‐Bendtsen, A. Kadziola, K. V. Mikkelsen, M. Brøndsted Nielsen, *Chem. – A Eur. J.* **2021**, *27*, 8315–8324.

[25] P. W. Antoni, C. Golz, M. M. Hansmann, *Angew. Chem. Int. Ed.* **2022**, *61*, e202203064.

[26] R. Kumar, P. J. Chmielewski, T. Lis, D. Volkmer, M. Stępień, *Angew. Chem. Int. Ed.* **2022**, *61*, e202207486.

[27] Y. Hayashi, S. Suzuki, T. Suzuki, Y. Ishigaki, *J. Am. Chem. Soc.* **2023**, *145*, 2596–2608.

[28] M. Hayakawa, N. Sunayama, S. I. Takagi, Y. Matsuo, A. Tamaki, S. Yamaguchi, S. Seki, A. Fukazawa, *Nat. Commun.* **2023**, *14*, 2741.

[29] Y. Ishigaki, T. Harimoto, K. Sugawara, T. Suzuki, *J. Am. Chem. Soc.* **2021**, *143*, 3306–3311.

[30] Y. Sakano, R. Katoono, K. Fujiwara, T. Suzuki, *Chem. Lett.* **2014**, *43*, 1143–1145.

[31] Y. Ishigaki, K. Sugawara, M. Yoshida, M. Kato, T. Suzuki, *Bull. Chem. Soc. Jpn.* **2019**, *92*, 1211–1217.

[32] T. Harimoto, T. Suzuki, Y. Ishigaki, *Chem. – A Eur. J.* **2023**, *29*, e202203899.

[33] S. Wang, J. Yuan, J. Xie, Z. Lu, L. Jiang, Y. Mu, Y. Huo, Y. Tsuchido, K. Zhu, *Angew. Chem. Int. Ed.* **2021**, *60*, 18443–18447.

[34] S. I. Etkind, T. M. Swager, *Synthesis (Stuttg).* **2022**, *54*, 4843–4863.

[35] M. Lin, L. Bian, Q. Chen, H. Xu, Z. Liu, K. Zhu, *Angew. Chem. Int. Ed.* **2023**, *62*, e202303035.

[36] M. Matsuoka, A. Iwamoto, T. Kitao, *J. Heterocycl. Chem.* **1991**, *28*, 1445–1447.

[37] M. J. Frisch, G. W. Trucks, H. B. Schlegel, G. E. Scuseria, M. A. Robb, J. R. Cheeseman, G. Scalmani, V. Barone, G. A. Petersson, X. Nakatsuji, H.; Li, M. Caricato, A. V. Marenich, J. Bloino, B. G. Janesko, R. Gomperts, B. Mennucci, H. P. Hratchian, J. V. Ortiz, A. F. Izmaylov, J. L. Sonnenberg, D. Williams-Young, F. Ding, F. Lipparini, F. Egidi, J. Goings, B. Peng, A. Petrone, T. Henderson, D. Ranasinghe, V. G. Zakrzewski, J. Gao, N. Rega, G. Zheng, W. Liang, M. Hada, M. Ehara, K. Toyota, R. Fukuda, J. Hasegawa, M. Ishida, T. Nakajima, Y. Honda, O. Kitao, H. Nakai, T. Vreven, K. Throssell, J. A. J. Montgomery, J. E. Peralta, F. Ogliaro, M. J. Bearpark, J. J. Heyd, E. N. Brothers, K. N. Kudin, V. N. Staroverov, T. A. Keith, R. Kobayashi, J. Normand, K. Raghavachari, A. P. Rendell, J. C. Burant, S. S. Iyengar, J. Tomasi, M. Cossi, J. M. Millam, M. Klene, C. Adamo, R. Cammi, J. W. Ochterski, R. L. Martin, K. Morokuma, O. Farkas, J. B. Foresman, D. J. Fox, *Gaussian 16, Revision B.01*, Gaussian, Inc., Wallingford CT, **2016**.

[38] O. V. Dolomanov, L. J. Bourhis, R. J. Gildea, J. A. K. Howard, H. Puschmann, *J. Appl. Crystallogr.* **2009**, *42*, 339–341.

[39] G. M. Sheldrick, *Acta Crystallogr. Sect. A Found. Adv.* **2015**, *71*, 3–8.

[40] G. M. Sheldrick, *Acta Crystallogr. Sect. C Struct. Chem.* **2015**, *71*, 3–8.

[41] Deposition numbers 2288937 [for **1a** (**F**-$F_{syn}$)], 2288938 [for **1a** (**F**-$F_{anti}$)], 2288939 [for **1b** (**F**-$F_{syn}$)], 2288940 [for $\mathbf{1a}^{4+}(SbCl_6^-)_4$], and 2288941 (for **3**) contain the supplementary crystallographic data for this paper. These data are provided free of charge by the joint Cambridge Crystallographic Data Centre and Fachinformationszentrum Karlsruhe Access Structures service.

## Entry for the Table of Contents

Insert graphic for Table of Contents here.

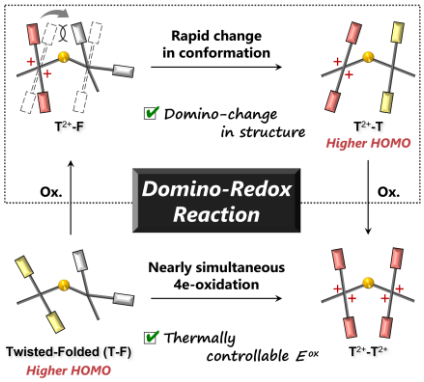


Domino-redox reaction was achieved by a facile apparent 2e-oxidation (trigger) of a thermally activated twisted-folded form of bisquinodimethane with a dithiin skeleton. After the formation of the dication, the steric repulsion and interelectrophore interaction cause a facile and rapid change in structure into the doubly twisted form, which facilitates the subsequent oxidation to the tetracation, resulting in the apparent 4e-oxidation (domino).

Institute and/or researcher Twitter usernames: Takashi Harimoto (@ZhangBen_dyrex), Yusuke Ishigaki (@ysk_isgk), and Laboratory (@Yuuichi_Hokudai)